Comparison on atomic/molecular layer deposition grown aluminum alkoxide polymer films using alkane and alkyne organic precursors

Cite as: J. Vac. Sci. Technol. A **36**, 01A108 (2018); https://doi.org/10.1116/1.4990776
Submitted: 17 June 2017 . Accepted: 23 October 2017 . Published Online: 17 November 2017

Devika Choudhury, Gopalan Rajaraman, and Shaibal K. Sarkar

Comparison on atomic/molecular layer deposition grown aluminum alkoxide polymer films using alkane and alkyne organic precursors

Devika Choudhury
Department of Energy Science and Engineering, Indian Institute of Technology Bombay, Mumbai 400076, India

Gopalan Rajaraman
Department of Chemistry, Indian Institute of Technology Bombay, Mumbai 400076, India

Shaibal K. Sarkar[a)]
Department of Energy Science and Engineering, Indian Institute of Technology Bombay, Mumbai 400076, India

(Received 17 June 2017; accepted 23 October 2017; published 17 November 2017)

Most hybrid films grown by atomic and molecular layer deposition (ALD and MLD) at relatively low temperatures commonly incorporate aliphatic organic bifunctional hydrocarbons as their organic counterparts. This often results in "double reactions" leading to lower growth rates, relatively poor film quality, and atmospherically unstable hybrid films. Although such a drawback has been overcome in the past using three-step ABC reactions, aromatic organic precursors, and heterobifunctional precursors, each has displayed one or the other limitations of growth. In this work, the possibility of overcoming double reactions during hybrid film growth by MLD at relatively low temperatures using an *sp*-hybridized carbon backbone organic precursor is explored. 1,4-butynediol (BDy) along with trimethylaluminum (TMA) is used to deposit "alucone" films at 80 °C. A comparison on growth and properties of the resultant film is drawn with another alucone film deposited using alkane based hydrocarbon, 1,4-butanediol (BD). *In situ* quartz crystal microbalance and fourier transform infrared (FTIR) spectroscopy studies are performed to determine and compare the growth and surface chemistry of the deposited films. Unfortunately, TMA-BDy films show similar growth characteristics to TMA-BD ones. A 2:1 stoichiometry of growth is observed not only for TMA-BD but also for TMA-BDy films. This shows the occurrence of double reactions irrespective of the carbon–carbon linkages for the linear homobifunctional organic precursors used. A detailed understanding of the stability issue of the deposited hybrid films is further obtained utilizing *ex situ* FTIR and x-ray reflectivity measurements in this work. *Published by the AVS.*
https://doi.org/10.1116/1.4990776

I. INTRODUCTION

Hybrids are a class of compounds in which the synergistic combination of inorganic and organic constituents results in innovative properties different from their parent counterparts.[1] Thus, the benefits of both worlds of chemistry are obtained in a single molecular composite in hybrid films. Organic-inorganic thin films possessing interesting properties due to their specific functionalities often find wide usage in various applications.[2,3] Hybrid films are used extensively as dielectric layers in thin film transistors, as charge trapping layers in memory devices, as photocatalytic layers, as gas barrier layers, etc.[4–10]

Although an attractive class of compounds, deposition of hybrid thin films puts forth quite a challenge due to the distinctly different physical and chemical characteristics of the organic and inorganic components involved.[11–13] The variety of possible applications not only demand an accurate thickness of the deposited films but also at various temperatures, often as low as room temperature in the case of flexible substrate applications. Over the last few years, the combination of atomic layer deposition (ALD) and molecular layer deposition (MLD) has successfully emerged as a distinctive method for depositing organic–inorganic hybrid thin films.[14–16] While ALD caters to the deposition of the inorganic constituents, MLD, a variant of ALD, involving molecules instead of atoms, is responsible for the incorporation of the organic counterpart into the single molecular chain in such hybrid films.[16,17] It is the sequential, self-limiting surface reaction of ALD and MLD that makes possible the growth of uniform, conformal, and pin hole free hybrid thin films on a variety of substrates with accurate thickness control.

The very first ALD/MLD hybrid film reported in the open literature is a poly(aluminum ethylene glycol) film using trimethylaluminum (TMA) and ethylene glycol (EG) as the inorganic and organic precursor, respectively.[18] The resulting polymer in the form $(\text{-O-Al-O-R})_n$ has since then been used as a reference for the growth of numerous other hybrid films. Most common amongst them are a group of metaloxide polymer films popularly known as the "metalcones."[14] The family of these metalcone films are developed using different metalorganic precursors coupled with various organic alcohols to form hybrid polymer chains. Depending on their inorganic centers, these films are named "alucones,"[18–20] zincones,[21–23] titanicones,[24] zircones,[25] etc.

The organic alcohols used for the development of metalcones are mostly homobifunctional linear carbon chains.

[a)]Electronic mail: shaibal.sarkar@iitb.ac.in

One of the drawbacks of such molecules is the probability of occurrence of "double reactions" during film growth.[18] These homobifunctional precursors like EG having weak rigidity tend to react twice with the surface sites, thus compromising growth of the hybrid chains. This not only decreases the growth rate of the resulting films but also hampers the film quality and stability.[18] Such a limitation is however overcome by utilizing a three-step ABC reaction involving a ring opening mechanism as reported by Yoon *et al*.[26] These chain opening reactions although result in a significantly higher growth rate of films but does so at the expense of complicating the deposition mechanism with the use of extra precursors. A comparative simpler solution if further obtained by using aromatic diols like hydroquinone.[21,22] Although homobifunctional in nature, the presence of a stiff benzene backbone prevents the possibility of the molecule to react twice in such cases.[27,28]

Aromatic homobifunctional organic precursor based hybrid films overcome the disadvantage of double reactions, however, at the expense of higher deposition temperatures[1,27] The extremely low vapor pressure of most of the aromatic organic precursors necessitating higher annealing temperature of the compounds limits the possibility of depositing hybrid films at lower temperatures. This restricts the applicability of the organic–inorganic films in various fields especially for temperature sensitive applications. Moreover, the instability issue of these hybrid films also poses to be a concern in terms of their applications in various domains.[29]

Thus, a trade-off between linear growth and higher growth rates and lower deposition temperature coupled with improved stability of hybrid films by ALD/MLD using homobifunctional organic precursors definitely needs to be explored further. We believe that one of the ways to achieve this aim is the possible usage of alkyne organic precursors. The alkyne molecules having an *sp*-hybridized carbon backbone can provide a better support avoiding bending of the organic molecules and subsequent double reactions, thus resulting in straight polymeric chains. Adequate vapor pressure obtained at relatively low annealing temperature allows low temperature deposition of these hybrid films, thus solving both the issues of growth rate and lower deposition temperature. In this work, aluminum alkoxide alucone films are grown using 1,4-butynediol (HO-C_4H_4-OH, BDy) along with trimethylaluminum. Growth characteristics of the resultant film are compared with those of another alucone film developed using an aliphatic organic diol, 1,4-butanediol (HO-C_4H_8-OH, BD), for comparing the growth chemistry of both types of linear organic precursors with different carbon linkages. The well-known atomistic reaction between a metalorganic precursor and a diol is also established using density functional theory (DFT) in this work. The growth characteristics including the self-limiting behavior of TMA and BD/BDy are studied using *in situ* quartz crystal microbalance (QCM). The change in surface-species during each half-cycle reaction is observed by means of *in situ* Fourier transform infrared (FTIR) spectroscopy measurements. *Ex situ* FTIR and x-ray reflectivity (XRR) measurements are further carried out in this work to study the stability of the resultant films in ambient.

II. EXPERIMENT

Alucone films are deposited in a hot walled viscous flow ALD reactor. The design of the reactor is similar to the one described by Elam *et al*. earlier.[30] TMA (Sigma Aldrich) is used as the aluminum source, while BD (Sigma Aldrich) and BDy (Sigma Aldrich) are used as the organic sources to deposit the hybrid films. All the precursors are used as received. While TMA is maintained at room temperature, the stainless steel bubbler retaining BD and BDy is heated to 80 and 50 °C, respectively. All the precursors are dosed into the reactor through differentially heated lines to avoid any unwanted condensation inside them. Due to the comparatively lower vapor pressure of BD and BDy, they are dosed into the reactor with the assistance of a carrier gas through an overhead gas assembly. Precursor doses are controlled using pneumatically controlled bellow valves and manual metering valves. All depositions are done in a laminar flow regime at a pressure of 0.9 Torr maintained inside the reactor with high purity N_2 flow, controlled by mass flow controllers (MKS). Here, N_2 is used both as the purging and the carrier gas.

During deposition, film growth is monitored using *in situ* QCM. An AT-cut gold coated polished crystal with a resonant frequency of 6 MHz (from Inficon) is used in a crystal drawer and retainer assembly and inserted into the reactor horizontally facing upward. Nonconducting silver epoxy is used to vacuum seal the crystal, thus preventing any precursor deposition on the backside of it. As a further precaution, an additional 0.1 Torr of N_2 flow is also maintained inside the reactor to prevent deposition on the crystal back. An Inficon SQM-160 thickness monitor is used to record the frequency change of the crystal during deposition of the film. This change in frequency is converted into mass gain using the Saurbrey equation.[31]

Surface chemistry during each ALD/MLD cycle of alucone deposition is studied employing *in situ* FTIR spectroscopy. Thin films are deposited on KBr pellets in a similarly equipped reactor as the previous one. In this arrangement, the beam from the IR source passes through a ZnSe window before falling on the substrate. The transmitted IR beam is then detected using an externally placed liquid N_2 cooled mercury cadmium telluride detector after passing through another ZnSe window. All the absorbance spectra are captured using a Vertex 70 instrument from Bruker over a range of 370 to 4000 cm^{-1}, with a resolution of 4 cm^{-1}, and averaged over 100 scans. *Ex situ* FTIR spectra for stability studies are also recorded in the same instrument but using an internally placed deuterated triglycine sulfate detector, over the same wavelength range.

III. RESULTS AND DISCUSSION

A. *In situ* QCM studies

A theoretical understanding on the atomistic reaction mechanism between TMA and BD/BDy is first attained from

DFT calculations. The potential energy surface diagrams obtained for the overall reaction of

$$(A)\ Al(CH_3)_3{}^* + OH - R - OH \rightarrow Al - O - R - OH* + CH_4,$$

where "R" represents C_4H_8 or C_4H_4 in this case for BD or BDy, respectively, and "*" stands for the surface species, show exothermic reactions for both, with minimal activation barrier involved [shown in Figs. S1(a) and S1(b) in the supplementary material].[32] This ascertains the feasibility of low temperature deposition of TMA-BD/BDy films.

Thus, an ideal TMA-BD/BDy growth reaction chemistry can be considered as depicted in the schematic in Fig. 1.

The overall reaction mechanism can be further divided into two half-cycle reactions known commonly for MLD deposition chemistry between a metal alkyl and an organic diol

$$(X)\ SOAl - OH^* + Al(CH_3)_3 \rightarrow SOAlO - Al(CH_3)_2{}^* + CH_4,$$
$$(Y)\ SOAlO - Al(CH_3)^* + OH - R - OH \rightarrow SOAlOAl - O - R - OH^* + CH_4,$$

where "S" denotes the starting substrate, R represents either C_4H_8 or C_4H_4 in this case, and * stands for the surface species.

In situ QCM is initially employed to attain the temperature window for alucone depositions following (X) and (Y) half cycle reactions. Figure 2 shows the temperature dependent mass gain of the deposited alucone films. A 1 s-30 s-1 s-30 s dose and purge sequence for alternate TMA and BD/BDy doses is utilized for the deposition of films. Although lower activation barrier energy is involved which necessitates considerably low thermal energy required for the completion of the reaction process, considering the annealing temperatures of the organic precursors, the minimum deposition temperature for both alucone films is kept at 80 °C and not lower.

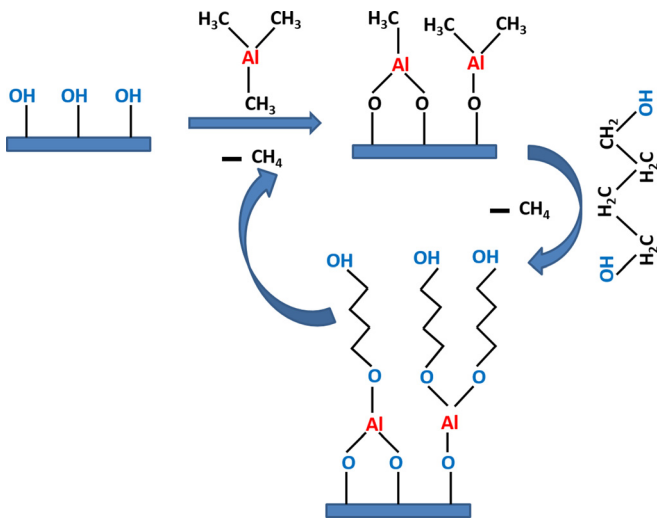

FIG. 1. (Color online) Probable reaction mechanism of alucone film growth using TMA and BD considering a 2:3 stoichiometry.

As seen from Fig. 2, the mass gain is found to decrease with the increasing deposition temperature, a trend visible for both the alucone films. Such a decrease in film growth at higher deposition temperatures is seen earlier in the case of other hybrid films as well.[23] This can be attributed to primarily two causes. On the one hand, while higher desorption of species from the substrate can result in lower growth, a more probable cause is the lower rate of organic precursor adsorption on the surface at higher temperatures, leading to a reduced growth rate. Thus, due to the maximum growth rate attained, henceforth all depositions are carried out at 80 °C for all further characterization of the alucone films.

The self-limiting nature of film growth is studied to confirm the occurrence of surface limited reactions of TMA and BD/BDy without any time dependent residual desorption occurring from the surface. Figure 3 shows mass gain versus number of doses of TMA and BD/BDy precursors.

(n × 1) s-30 s-1 s-30 s and 1 s-30 s-(m × 1) s-30 s dosing sequences are utilized for studying the self-limiting behavior of TMA and BD(or BDy). Here, "n" and "m" are the number of doses of TMA and BD(or BDy), respectively. As seen from Fig. 3(a), in the case of the TMA-BD alucone film, five consecutive 1 s TMA doses corresponding to 3×10^4 L result in the self-saturation of the precursor. Similarly, saturation is obtained with five consecutive 1 s doses of BD as well. For TMA-BDy on the other hand, a single dose of TMA (6×10^4 L) results in a saturated growth. BDy however requires five or more 1 s doses to get saturated. No further increase in mass gain is observed on further exposure of the surface to subsequent precursor doses, thus validating the self-limiting criteria for the ALD/MLD reaction between TMA and BD as well as TMA and BDy. This satisfies the primary criterion of ALD/MLD growth.

Furthermore, the growth nature of the hybrid films is observed also by *in situ* QCM. A linear growth of both alucone films is observed at 80 °C as shown in Fig. 4, over a seeding layer of Al_2O_3.

The total mass gain for 100 cycles of TMA-BD is found to be ca. 2340 ng/cm^2. This gives an average mass gain of 23.40 ng/cm^2 per cycle. TMA-BDy alucone films are also found to have similar growth behavior with a negligible difference in the average mass gain per cycle being

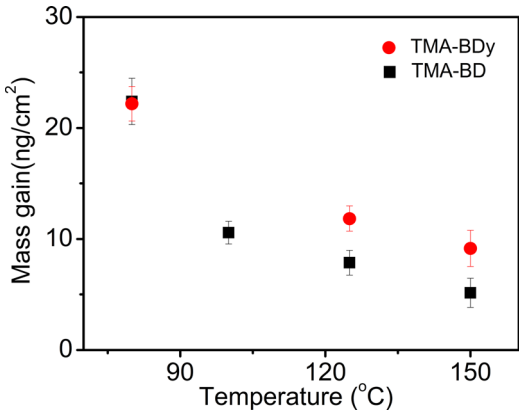

FIG. 2. (Color online) Mass gain vs deposition temperature for TMA-BD and TMA-BDy as measured by *in situ* QCM.

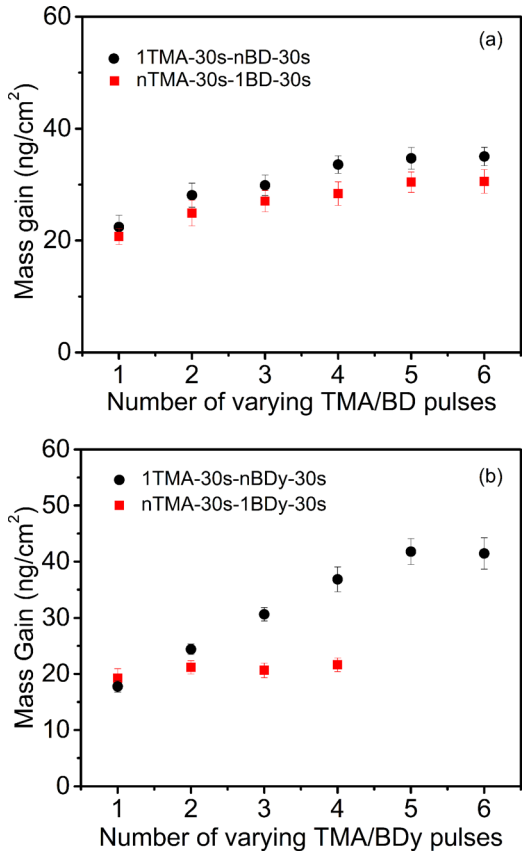

FIG. 3. (Color online) Self-limiting behavior of (a) TMA and BD precursors and (b) TMA and BDy precursors measured using *in situ* QCM during alucone deposition.

approximately 24 ng/cm^2. Considering the density of the materials to be ca. 1.7–1.8 gm/cm^3, as attained from XRR measurements (as shown in Fig. S2 in the supplementary material), a growth rate of 0.8–0.9 Å/cycle is obtained. This is significantly lower than other alucone films developed earlier.[18,27] That the presence of single carbon bonds in BD might cause double reactions during TMA-BD alucone growth thus leading to lower growth is expected. However, such a low growth rate for the *sp*-hybridized carbon linkage containing TMA-BDy films is unexpected and in contrast to the initial belief of this work. Considering the chain length

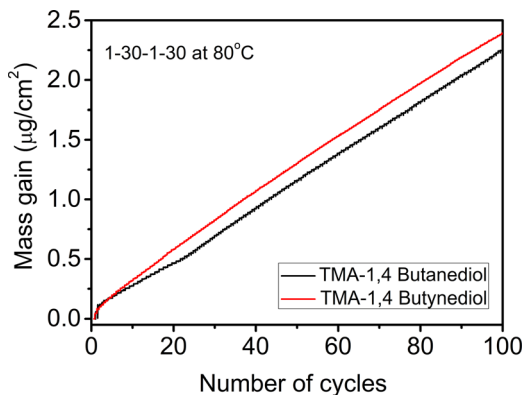

FIG. 4. (Color online) Linear growth for 100 cycles of alucone films deposited at 80 °C.

of BDy molecules, such a growth rate is found to be much lower than that of the expected values for linear growth of a single monolayer of film. This indicates the tendency of both TMA-BD and TMA-BDy film formation dissimilar to the ideal scenario as shown in Fig. 1.

To further understand the cause behind the relatively low growth rate of both the alucone films, closer inspection of the growth characteristics of the aliphatic organic precursor based alucone films is carried out. A significant difference in mass gain between the nucleation and the steady state region of growth of both alucone films on the Al_2O_3 surface is observed at 80 °C. Similar growth characteristic features are obtained independent of temperature. Figures 5(a) and 5(c) and Figs. 5(b) and 5(d) show the first alucone cycle on the Al_2O_3 seed layer and few of the later cycles in the linear growth regime of TMA-BD and TMA-BDy film depositions, respectively.

It is found from Fig. 5 that a large positive mass gain is observed in the first cycle of TMA-BD/BDy growth. Mass gains of 108.46 and 80.27 ng/cm^2 are obtained during the first TMA-BD and TMA-BDy cycles, respectively. This is followed by a considerable decrease in the steady state linear growth regime. Almost a 1/5th and 1/4th decrease in the mass is observed. An average mass gain of approximately 22–23 ng/cm^2 is obtained during the steady state growth regime of both alucone films. In the case of the absence of reactive surface sites due to surface poisoning during the initial cycles of growth, such a decrease in mass gain can be seen in the later growth cycles. This definitely hints toward the possibility of occurrence of double reactions for both aliphatic diols, irrespective of the nature of their carbon-carbon bonds, during film growth.

B. *In situ* FTIR studies

The possibility of double reactions as seen from *in situ* QCM is further confirmed by studying the surface reactions occurring in the initial few cycles of alucone growth on the Al_2O_3 surface by employing *in situ* FTIR studies. The TMA-BDy difference FTIR spectra are demonstrated to show the possibility of double reactions in the case of alkyne diols, in contrast to the initial assumption. Figure 6 shows the FTIR difference spectra of TMA-H_2O and TMA-BDy for alucone growth over the Al_2O_3 surface.

100 cycles of Al_2O_3 are performed on KBr pellets initially. Each of the spectra here is a difference spectrum obtained with reference to its previous one. The positive peaks denote the presence of the particular species, while the negative ones denote the absence due to its removal from the surface. For clarity in presentation, all spectra are shown between only 2500 and 3700 cm^{-1}. Changes in the FTIR peaks are obtained as expected as shown for the last ALD Al_2O_3 cycle. After saturated TMA dosages, a positive CH stretch is observed at 3016 cm^{-1} with a simultaneous inversion of the OH stretch at 3400 cm^{-1}. Subsequent H_2O dosages show an appearance and disappearance of OH and CH stretches, respectively, thus confirming the growth of the Al_2O_3 film. This is immediately followed by the deposition

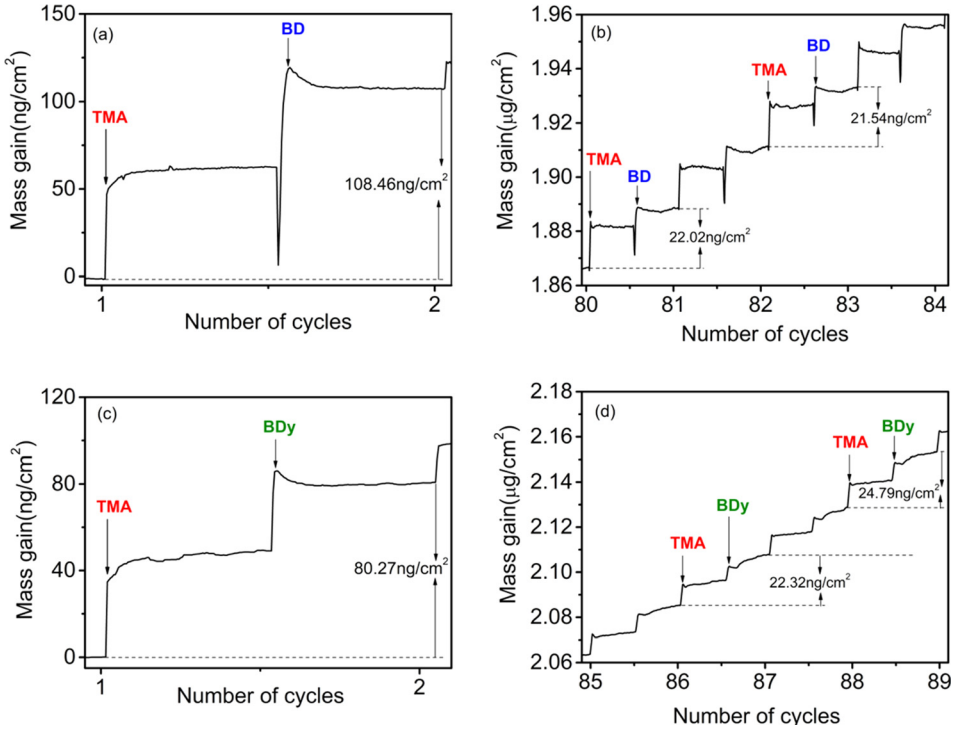

FIG. 5. (Color online) Mass gain measured by *in situ* QCM during (a) first TMA-BD cycle, (b) linear growth regime of TMA-BD, (c) first TMA-BDy cycle, and (d) linear growth regime of TMA-BDy.

of TMA-BDy cycles. The TMA-1 spectrum is identical to the TMA spectrum as expected. Subsequent BDy dosages result in the disappearance of the CH stretch at 3016 cm^{-1} with the simultaneous appearance of symmetric and asymmetric stretching CH_2 vibrations at 2907 and 2857 cm^{-1}, respectively, as seen from the BDy-1 spectrum in Fig. 6. The CH_2 stretches are signatures for the BDy molecule. However, no significant positive appearance of OH is found after the dosing of BDy (BDy-1). This continues in the same manner for the consecutive alucone cycles. As a result, the fifth TMA pulsing also does not display any discernible negative OH stretch. The absence of the complete replacement of surface sites during each half-cycle reaction validates the lower growth rate recorded by QCM as described previously. Similar observation is recorded for TMA-BD films which can be well attributed to the occurrence of double reactions as earlier reported for metalcone films.[18,23] However, the fact that TMA-BDy films also result in similar growth features shows the failure to overcome double reactions using *sp*-hybridized carbon containing homobifunctional organic precursor molecules. This definitely shows that during the first cycle itself, the organic molecule undergoes possible double reactions, thus validating the earlier QCM results. A detailed study on the flip-flop of different signature vibrational peaks during alucone growth is provided in Fig. S3 in the supplementary material.

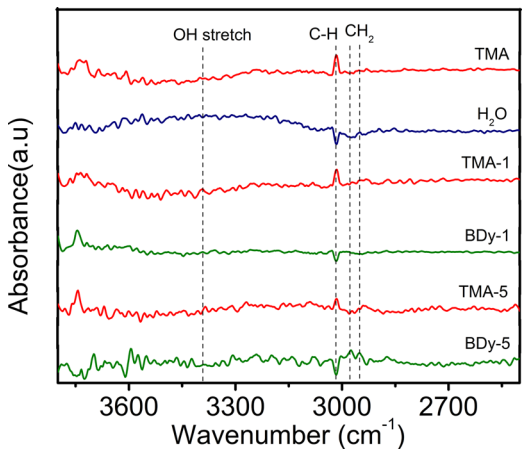

FIG. 6. (Color online) *In situ* FTIR spectra of the last TMA-H_2O cycle and the first and fifth TMA-BDy cycles.

The occurrence of double reactions during film growth further gives rise to probabilities of adsorption of TMA molecules in the near surface region of the hybrid polymer films. The progressive growth of TMA-BD and TMA-BDy alucone films is observed by recording the FTIR spectra after each 100 cycles of alucone deposition till 500 cycles of the films. Figures 7(a) and 7(b) show the frequency spectrum as recorded by FTIR, depicting the linear growth of both TMA-BD and TMA-BDy alucone films.

All the absorbance spectra are recorded with the bare KBr pellet as the background reference. The progressive increase in the absorbance intensity of the C-H, C-C, and C-O signature peaks justifies the linear growth of alucone films. All the observed vibrational features can be considered as the signature peaks for aluminum alkoxide polymer chains. Both the experimentally obtained absorbance spectra closely match the spectrum generated using density functional theory calculations as well. This confirms the assignment of the vibrational features against the signature peaks.

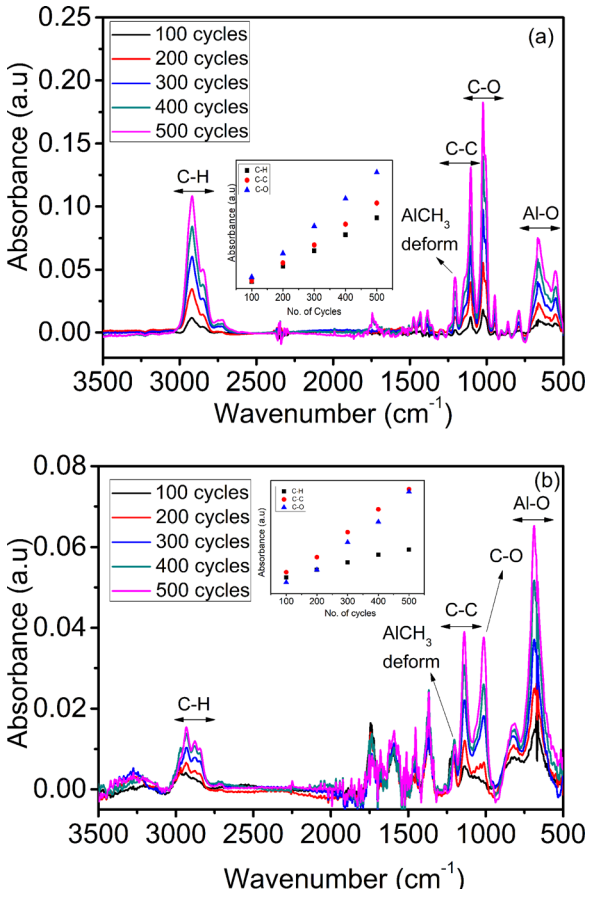

FIG. 7. (Color online) Vibrational spectra of (a) TMA-BD and (b) TMA-BDy with an increase in the number of deposition cycles.

Prominent absorbances observed in Fig. 7 at 3000–2800 cm^{-1} correspond to the C-H stretching vibrations from the ($O\text{-}CH_2CH_2CH_2CH_2\text{-}O$) or ($O\text{-}CH_2CCCH_2\text{-}O$) linkage in the polymer. C-C and C-O stretches are found at 1100 and 1020 cm^{-1}, respectively. Due to the very low absorbance intensity of C≡C, no discernible peak is observed for that particular bonding in Fig. 7(b). The presence of a peak at around 650 cm^{-1} is due to the Al-O stretching vibration in the alucone films. Smaller absorbances corresponding to CH_2 scissors and wag modes are also found between 1300 and 1500 cm^{-1}.

Apart from the negligible absorbance around 3000–3500 cm^{-1} which denotes the absence of the prominent O-H stretch, the presence of a prominent feature at 1201 cm^{-1} for both TMA-BD and TMA-BDy alucone films is noteworthy here. This peak can be attributed to the Al-CH_3 deformation which may be due to the presence of unreacted TMA in the near surface regions of the hybrid alucone films. This definitely suggests that the complete removal of the CH_3 species does not occur after BD/BDy dosages, thus leading to the entrapment of unreacted Al-CH_3* species in the bulk of the material.

The presence of unreacted Al-CH_3* is also confirmed by studying the self-saturation of TMA and BD from *in situ* FTIR measurements (Fig. S4 in the supplementary material). This lack of complete reaction and removal of Al-CH_3* species can be attributed to the diffusion limitations or steric hindrance of BD and BDy molecules. That the absorbance peak at around 1200 cm^{-1} is due to the presence of TMA is further confirmed from the fact that on continuous H_2O dosing on the film, the deformation peak completely disappears with time. H_2O being a molecule smaller in size than BD/BDy can obviously enter the limited spaces between the TMA-BD/TMA-BDy polymer chains and react with the unreacted Al-CH_3* surface sites, thus resulting in the disappearance of that particular vibrational peak. This is however not the case in the case of repeated BD/BDy pulsing, showing that BD or BDy is not able to completely react with the existing Al-CH_3 surface species.

This possibility of the double reactions taking place during film growth thus leads to the probability of a reaction mechanism different from an ideal one as depicted in Fig. 1. As described in an earlier report for TMA/Glycidol alucone films, in this work also, the stoichiometry of TMA:BD and TMA:BDY can be calculated from the following relation:[19]

$$\Delta M_{TMA}/(\Delta M_{TMA} + \Delta M_B) = x.(M_{TMA})/(x.M_{TMA} + y.(M_B - M_{CH_4})).$$

Here, M_{TMA}, M_B, and M_{CH_4} are the molar masses of TMA, butanediol or butynediol, and the by-product methane, respectively. For a 2:3 TMA/BD stoichiometry, the said ratio would be approximately 0.4. The mass gain of 108.46 ng/cm^2 obtained from *in situ* QCM as shown in Fig. 5(a) in the very first XY cycle of TMA-BD results in a ratio of $\Delta M_{TMA}/(\Delta M_{TMA} + \Delta M_{BD})$ of approximately 0.5. Although not exactly accurate, this moderately close similarity between the ideal and observed values shows that TMA and BD are likely to react at a 2:3 ratio during the first MLD cycle of alucone deposition. In the linear regime, on the other hand, the average ratio obtained from the mass gains of 22 ng/cm^2 as seen in Fig. 5(c) is 0.65 which corresponds to a TMA/BD stoichiometry of 2:1. Such a discrepancy in stoichiometry between the first and later cycles of the alucone film points toward the occurrence of two probable reactions during the MLD growth. First, two molecules of TMA may react with a single BD molecule, thus explaining the probable double reactions taking place. Or, an Al_2O_2 dimeric core can be formed due to the TMA reaction with BD. Here, the most probable option however seems to be the first one as this explains the presence of unreacted methylene deformation features as observed in the bulk material from FTIR measurements. Similar values are also attained for the TMA-BDy films as well. Thus, the modified schematic can be represented as shown in Fig. 8.

The 2:1 stoichiometry thus also explains the relatively low growth rate of the alucone films. Although expected in the case of TMA-BD films, the possibility of overcoming the double reactions using BDy molecules with C≡C linkage to provide support to the polymer chain for the growth of alucone films thus fails here.

C. Stability studies

Occurrence of double reactions not only results in the low growth rate of the films but also affects the stability of the

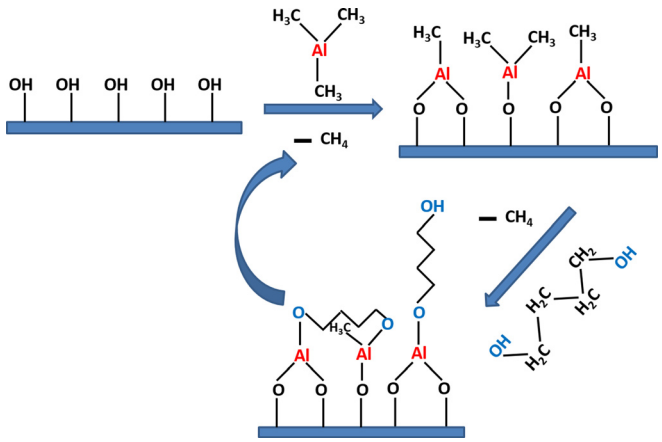

FIG. 8. (Color online) Probable reaction mechanism of alucone film growth using TMA and BD considering a 2:1 stoichiometry.

grown hybrid films in air. The presence of unreacted Al-CH_3 makes these alucone films highly susceptible to the action of ambient moisture. Figure 9 shows a comparison in the FTIR spectrum of both alucone films recorded *in situ* and on immediate exposure to the ambient measured *ex situ*.

As evident, for both the films, exposure to the ambient results in immediate changes in the chemical nature of the films. This is likely due to the diffusion of atmospheric H_2O into the films, which reacts with the unreacted TMA species. The Al-CH_3 deformation completely disappears in the case of TMA-BDy, while a significant reduction is observed for TMA-BD films. Thus, a slight difference in the rate of degradation of the films can be observed. This can be due to the difference in the volume of unreacted TMA in the bulk of the polymer films as seen earlier from *in situ* FTIR, being higher for TMA-BD and lower for TMA-BDy films. This decrease in absorbance intensities is however not continuous. The changes occur either immediately or during the initial few hours of exposure, after which no significant change takes place as is evident from the time dependent FTIR and XRR measurements as shown in Fig. 10.

No changes are found on the other hand for the samples if kept in vacuum for the same time period. Capping of the alucone films with approximately 100 cycles (10 nm) of Al_2O_3 also does not result in completely preventing the absorption of moisture in the material. The stability issue thus still persists to be a major concern for alucone films in this work as well.

IV. SUMMARY AND CONCLUSIONS

Alucone films are deposited by molecular layer deposition using TMA as the inorganic source and two organic sources, 1,4-butynediol and 1,4-butanediol at 80 °C. The presence of *sp*-hybridization in alkyne 1,4-butynediol is believed to provide a possibility of overcoming the double reactions which were expected to occur for alkane 1,4-butanediol based films.

The self-limiting growth behavior of the precursors confirms the ALD/MLD type growth of both alucone films. Under deposition conditions of 80 °C temperature and 30 s

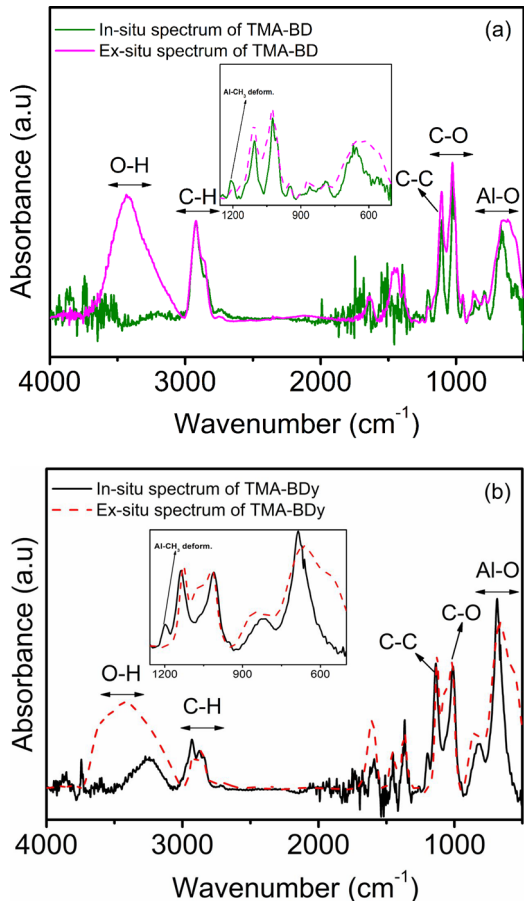

FIG. 9. (Color online) *In situ* and *ex situ* FTIR spectra of (a) TMA-BD and (b) TMA-BDy alucone films.

purge time, a growth rate as low as 0.8–0.9 Å/cycle is observed for both TMA-BD and TMA-BDy films using *in situ* QCM and XRR measurements. This is in contrast to the higher growth rate as expected for TMA-BDy films in the case of linear growth without any double reactions occurring. Further, stoichiometric calculations based on the $\Delta M_{TMA}/(\Delta M_{TMA} + \Delta M_{BD\ or\ BDy})$ ratio show that although film growth follows a 2:3 stoichiometry during the first deposition cycle, a 2:1 stoichiometry of film growth is observed in the linear regime of both the films. *In situ* FTIR measurements showing the absence of any significant flip-flop of OH stretch during each half cycle of the alucone films validate the resultant lower growth rates. Thus, despite linear growth of the alucone films, both deposition chemistries show probabilities of occurrence of double reactions during film growth irrespective of the nature of carbon bonds in their aliphatic organic constituents, thus contradicting the original belief.

The occurrence of double reactions results in the entrapment of unreacted TMA in the bulk of the alucone films, which renders the films unstable in ambient. The volume of unreacted TMA in TMA-BDy films is however observed to be lower than that in TMA-BD films. This results in the marginally improved stability of the TMA-BDy alucone films in atmosphere. The difference in the presence of unreacted TMA in the bulk of the films although suggests the

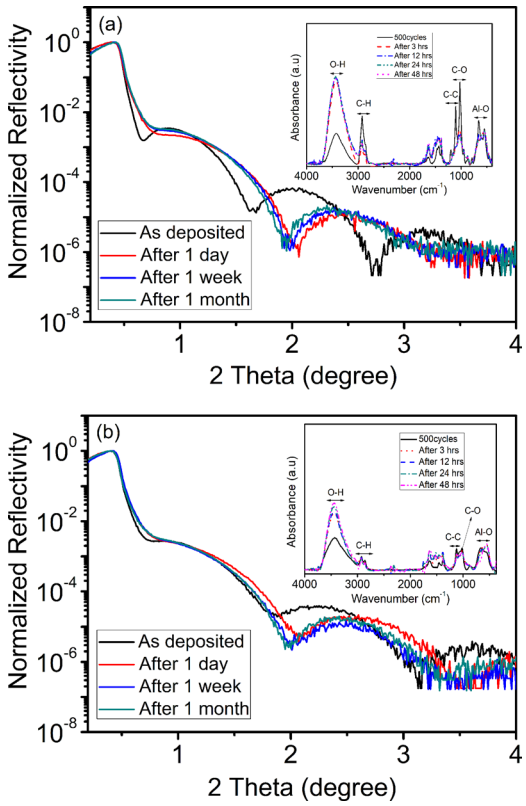

FIG. 10. (Color online) Comparison of thickness and chemical nature of (a) TMA-BD and (b) TMA-BDy alucone films on continuous exposure to the ambient as measured by XRR.

possibility of lesser double reactions occurring during growth of the alkyne based alucone films as compared to alkane ones, the lack of any definite proof remains. The fact that a significantly low growth rate is obtained also contradicts the above possibility. A detailed theoretical understanding of the growth mechanism of the films using surface DFT calculations can throw significant light on this contradiction and definitely remains a scope for future. Thus, it is found that although aliphatic organic based hybrid films have an advantage of lower deposition temperature over aromatic ones, the possibility of double reactions remains irrespective of the nature of carbon bonds in them. Whether any other AB chemistry utilizing homobifunctional organic precursors would provide a solution for the development of hybrid films at relatively low deposition temperature overcoming the double reactions still remains to be seen.

ACKNOWLEDGMENTS

This paper is based upon the work supported in part by the Solar Energy Research Institute for India and the United States (SERIIUS), funded jointly by the U.S. Department of Energy (under Subcontract No. DE-AC36-08GO28308) and the Government of India's Department of Science and Technology (under Subcontract No. IUSSTF/JCERDCSERIIUS/2012). The authors also acknowledge IIT Bombay for the computational facilities used in this work.

[1]A. Sood, P. Sundberg, and M. Karppinen, Dalton Trans. **42**, 3869 (2013).
[2]K. Gregorczyk and M. Knez, Prog. Mater. Sci. **75**, 1 (2016).
[3]M. Vähä-Nissi, P. Sundberg, E. Kauppi, T. Hirvikorpi, J. Sievänen, A. Sood, M. Karppinen, and A. Harlin, Thin Solid Films **520**, 6780 (2012).
[4]B. H. Lee, K. K. Im, K. H. Lee, S. Im, and M. M. Sung, Thin Solid Films **517**, 4056 (2009).
[5]B. H. Lee, K. H. Lee, S. Im, and M. M. Sung, Org. Electron. **9**, 1146 (2008).
[6]S. H. Cha, A. Park, K. H. Lee, S. Im, B. H. Lee, and M. M. Sung, Org. Electron. **11**, 159 (2010).
[7]W. Zhou, J. Leem, I. Park, Y. Li, Z. Jin, and Y.-S. Min, J. Mater. Chem. **22**, 23935 (2012).
[8]S. Ishchuk, D. H. Taffa, O. Hazut, N. Kaynan, and R. Yerushalmi, ACS Nano **6**, 7263 (2012).
[9]M. Yu, H. H. Funke, R. D. Noble, and J. L. Falconer, J. Am. Chem. Soc. **133**, 1748 (2011).
[10]A. Sood, P. Sundberg, J. Malm, and M. Karppinen, Appl. Surf. Sci. **257**, 6435 (2011).
[11]D. B. Mitzi, Chem. Mater. **13**, 3283 (2001).
[12]K. B. Blodgett, J. Am. Chem. Soc. **57**, 1007 (1935).
[13]G. Cao, H. G. Hong, and T. E. Mallouk, Acc. Chem. Res. **25**, 420 (1992).
[14]S. M. George, B. H. Lee, B. Yoon, A. I. Abdulagatov, and R. A. Hall, Nanosci. Nanotechnol. **11**, 7948 (2011).
[15]B. H. Lee, B. Yoon, A. I. Abdulagatov, R. A. Hall, and S. M. George, Adv. Funct. Mater. **23**, 532 (2013).
[16]P. Sundberg and M. Karppinen, Beilstein J. Nanotechnol. **5**, 1104 (2014).
[17]M. Leskala and M. Ritala, *Handbook of Thin Film Materials*, edited by H. S. Nalwa (Academic, New York, 2002), Vol. 1, Chap. 2.
[18]A. A. Dameron, D. Seghete, B. B. Burton, S. D. Davidson, A. S. Cavanagh, J. A. Bertrand, and S. M. George, Chem. Mater. **20**, 3315 (2008).
[19]Y. Lee, B. Yoon, A. S. Cavanagh, and S. M. George, Langmuir **27**, 15155 (2011).
[20]B. Gong, Q. Peng, and G. N. Parsons, J. Phys. Chem. B **115**, 5930 (2011).
[21]Q. Peng, B. Gong, R. M. VanGundy, and G. N. Parsons, Chem. Mater. **21**, 820 (2009).
[22]B. Yoon, B. H. Lee, and S. M. George, J. Phys. Chem. C **116**, 24784 (2012).
[23]B. Yoon, J. L. O'Patchen, D. Seghete, A. S. Cavanagh, and S. M. George, Chem. Vap. Deposition **15**, 112 (2009).
[24]A. I. Abdulagatov, R. A. Hall, J. L. Sutherland, B. H. Lee, A. S. Cavanagh, and S. M. George, Chem. Mater. **24**, 2854 (2012).
[25]B. H. Lee, V. R. Anderson, and S. M. George, Chem. Vap. Deposition **19**, 204 (2013).
[26]B. Yoon, D. Seghete, A. S. Cavanagh, and S. M. George, Chem. Mater. **21**, 5365 (2009).
[27]D. Choudhury, N. Mahuli, and S. K. Sarkar, J. Vac. Sci. Technol., A **33**, 01A115 (2015).
[28]D. Choudhury and S. K. Sarkar, Chem. Vap. Deposition **20**, 130 (2014).
[29]D. Choudhury, G. Rajaraman, and S. K. Sarkar, RSC Adv. **5**, 29947 (2015).
[30]J. W. Elam, M. D. Groner, and S. M. George, Rev. Sci. Instrum. **73**, 2981 (2002).
[31]G. Sauerbrey, Z. Phys. **155**, 206 (1959).
[32]See supplementary material at http://dx.doi.org/10.1116/1.4990776 for DFT calculations, additional XRR and FTIR measurement results.